2019

# Spag17 Deficiency Impairs Neuronal Cell Differentiation in Developing Brain

Olivia J. Choi
*Virginia Commonwealth University*

*Spag17* **Deficiency Impairs Neuronal Cell Differentiation in Developing Brain**

A thesis submitted in partial fulfillment of the requirements for the degree of Master of Science in Physiology and Biophysics at Virginia Commonwealth University

By

Olivia Jeong Min Choi

George Mason University, B.S. Forensic Science, 2016

Principal Investigator: Maria E. Teves Ph.D.

Department of Obstetrics and Gynecology

Virginia Commonwealth University

Richmond, Virginia

May, 2019

## Table of Contents

Acknowledgement

First and foremost, the completion of this thesis could not have been possible without the expertise, guidance and kindness of my mentor and advisor, Dr. Maria Teves. I would like to express my sincerest gratitude for the opportunities she has given me to work on her one-of-a-kind in the world project and experience the world of research.

I would also like to offer my special thanks to Dr. Jennifer Wolstenholme and Dr. Javier Gonzalez-Maeso for being my committee members, their encouragement, time and patience to go through lot of paperwork because of me.

I really appreciate the help from Sonya Washington for teaching me how to use microtome; Dr. Scott Walsh, for letting me use his microscope and cellSens program; Megan Sayyad, for teaching me how to perform tissue collection and cell culture; and Abdul and Gervyn for their work on β-Gal assay. Also thank you to Dr. Carmen Sato-Bigbee for guiding me on oligodendrocytes and cell cultures.

Thank you, Pam and Vita from Massey Cancer Center, for enduring through countless brain samples for me and ever-helpful teacher for my immunohistochemistry.

I could not ask for better lab mates than amazing Rewa Kulkarni and brilliant Paulene Sapao. They have patiently endured through my "Do you know where pipette/scissor/tubes are at?" and "Have you seen my pen/calculator/phone?" questions fifty times a week, and taught me how to be not afraid and learn from mistakes. Wherever we will end up, I will cherish our memories.

I would like to thank my family, VCU friends, and Alex Hirsch for constantly reminding me that Starbucks Frappuccino is not and never should be a meal replacement, and providing me with their care and love.

Last but not least, thank you, grandfather, for all of the memories you have given me. You'll be in my heart forever.

List of Figures

Abbreviations

ABC = Avidin-Biotin Complex

β-Gal = Beta-galactosidase

CMV-Cre = Cytomegalovirus-Cre

CNS = Central Nervous System

CP = Cortical Plate

CPC = Central Pair Complex

CSF = Cerebrospinal Fluid

DAB = 3,3'-Diaminobenzidine

diH2O = Distilled Water

E15.5 = Embryonic day 15.5

EtOH = Ethanol

FLP = Flippase

FRT = Flippase Recognition Target

GFAP = Glial Fibrillary Acidic Protein

GSK-3 = Glycogen Synthase Kinase-3

GWAS = Genome-Wide Association Studies

IF = Immunofluorescence

IHC = Immunohistochemistry

IZ = Intermediate Zone

KO = Knockout

LacZ = β -galactosidase encoding Lac Operon

LGE = Lateral ganglionic eminence

LoxP = Lox-flanked cassette

MGE = Medial ganglionic eminence

MRI = Magnetic Resonance Imaging

MZ = Marginal Zone

NeuN = Neuronal Nuclei / Fox-3

NSC = Neural Stem Cell

OPC = Oligodendrocyte Progenitor Cells

P0 = Postnatal day 0

PBS = Phosphate-buffered saline

PCD = Primary Ciliary Dyskinesia

R1 = Rhombomere 1

RGC = Radial Glial Cells

SEM = Standard error of the mean

SGZ = Subgranular Zone of the Dentate Gyrus

HH signaling = Hedgehog signaling

*Spag6* = Sperm-associated antigen-6

*Spag17* = Sperm-associated antigen-17

SVZ = Subventricular Zone

Trypsin-EDTA = Trypsin- ethylenediaminetetraacetic acid

Tuj1 = Neuron-Specific Class III β-tubulin

WT = Wild-type

VZ = Ventricular Zone

X-Gal = 5-Bromo-4-chloro-3-indolyl-beta-D-galactopyranoside

ABSTRACT

*Spag17* **DEFICIENCY IMPAIRS NEURAL CELL DIFFERENTIATION IN DEVELOPING BRAIN**

By Olivia Jeong Min Choi, B.S.

A thesis submitted in partial fulfillment of the requirements for the degree of Master of Science at Virginia Commonwealth University

Virginia Commonwealth University, 2019

Advisor: Maria E. Teves, Ph.D.
Department of Obstetrics and Gynecology

The development of the nervous system is a multi-level, time-sensitive process that relies heavily on cell differentiation. However, the molecular mechanisms that control brain development remain poorly understood. We generated a knockout (KO) mouse for the cilia associated gene *Spag17*. These animals develop hydrocephalus and enlarged ventricles consistent with the role of *Spag17* in the motility of ependymal cilia. However, other phenotypes that cannot be explained by this role were also present. Recently, a mutation in *Spag17* has been associated with brain malformations and severe intellectual disability in humans. Therefore, we hypothesized that *Spag17* plays a crucial role in nervous system development. To investigate this possibility, we first characterized the spatiotemporal expression of *Spag17* in the developing brain by using Beta-galactosidase staining and immunohistochemistry. Results showed *Spag17* expression in the spinal cord in embryonic E11. By E11.5-12.5 the expression extends to the rhombic lip from the developing hindbrain, as well as to the forebrain and midbrain regions. E14.5-15.5 embryos

exhibit an intense expression in the developing ventricles as well as the cerebellum. From E17.5

to birth (P0), the gene is more broadly expressed. We then used a global *Spag17* KO mouse

model to characterize the function of *Spag17* during brain development. Immunohistochemical

studies performed in brain sections from E15.5 and P0 time points showed increased expression

of the neural progenitor marker Nestin, and reduced expression of mature neuron marker NeuN,

increasing positive trend with the young neuron marker Tuj1. Altogether, these findings reveal

that *Spag17* has a unique spatiotemporal distribution and may be critical for the maturation of

neural progenitor cells.

.

Chapter 1: Introduction

1) Neurodevelopment and cell differentiation

The development of central nervous system (CNS) and brain is a highly complex process involving cascades of molecular signaling and cellular differentiation (1-3). During early developmental phase, neuroepithelial cells or neural stem cells (NSC) undergo proliferation via symmetrical division to generate two identical daughter stem cells to increase their number. Later on, NSCs start losing multipotency and differentitate in either asymmetrical or symmetrical cell division to produce one daughter stem cell with a differentiated cell or two differentiated cells (1-2). It has been reported that mutations of genes that disrupt this transition between proliferative symmetrical and differentiative asymmetrical division at the germinal zone can affect the cortical size (3-7). Persisting defects in NSC division can result in neurodevelopmental disorders such as microcephaly (reduced brain size) or megalocephaly (enlarged brain size) that can affect the brain size and intellectual capacity associated with it (4, 7-8). It has been also noted that dysregulation in neurogenesis and maturation has been observed in brains of autistic patients, with heavier and bigger brain and excess number of neurons in the frontal cortex (9-11).

2) Early structural development of brain

Gastrulation phase starts the transition from blastula to gastrula around embryonic day 6 (E6) after the conception for mouse, with tissue invagination to initiate epiblast cell migration and differentiation into three distinct stem cell lineage and body axis patterning (1, 12-13). Those cells who migrate into the deepest layer into primitive streak will form endodermal stem cell layer, which will later give rise to gut and respiratory tract organs. The layer right above the endoderm layer will become mesoderm and will later give rise to muscle, bone, cartilage, and the

vascular system. Lastly, the outermost layer will become ectoderm to give rise to skin, nails, sweat glands and CNS (1) (Figure 1). A subpopulation of ectoderm cell layer will receive additional signaling from the notochord, a cylinder of mesodermal cell aggregation, will differentiate into NSC and become a neuroectoderm layer to give rise to majority of CNS (12) (Figure 2).
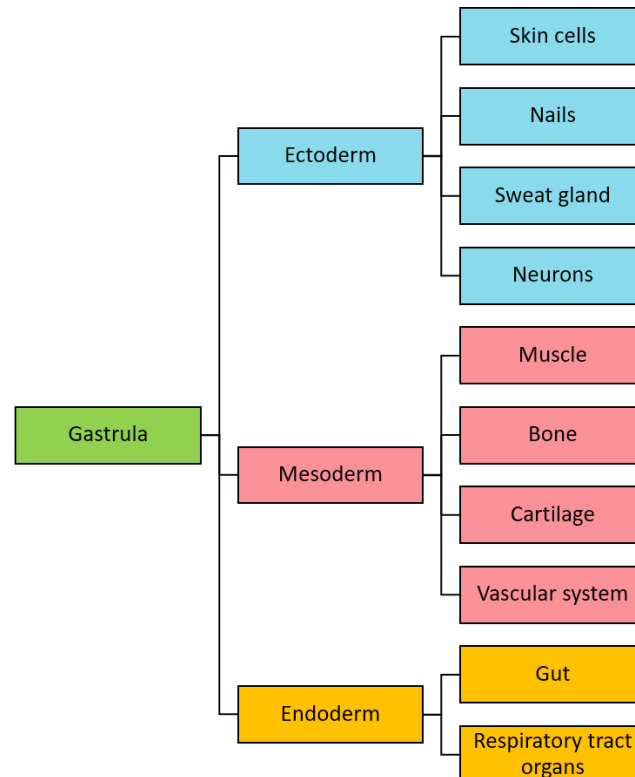


**Figure 1: Three primary cell layers and their derivation.** From gastrula, three germ cell layers form to give rise to various organs and cell types (1, 12-13)

During the neurulation process, the neuroectoderm will continue to proliferate until they become neural plate, and eventually fold into neural tube that acts as first brain structure and primitive form of spinal cord (1, 13) (Figure 2). From this hollow cylinder organ formation, the cavities of neural tube will become primitive ventricular system of the brain, which leads to calling the most apical cell layer next to the ventricles with the highest number neural progenitor cell bodies as ventricular zone (VZ) (1-3). As the neural tube closes and increases in size and

complexity throughout the development, three primary pouches or vesicles are assembled: prosencephalon (forebrain), mesencephalon (midbrain), and rhombencephalon (hindbrain). The most anterior forebrain will later become telencephalon (cerebrum) and diencephalon (thalamus, hypothalamus), mesencephalon in the middle will become midbrain, and most posterior hindbrain will give rise to medulla, pons and cerebellum (1). Before hindbrain fully becomes cerebellum, they segment into units called rhombomeres, and form assembly of rhombomeres called rhombic lip. The rhombic lip includes most anterior segment called rhombomere 1, which will be the major source of cerebellar granule cell precursors that will eventually give rise to more than half of the neurons in the adult brain (14-15). Also, during the folding of neural tubes, a specialized cell group called neural crest cells will be generated, and migrate away farther than other cell layers to give rise to diverse cell progeny including bone, cartilage and melanocytes of skin (1, 13) (Figure 2).
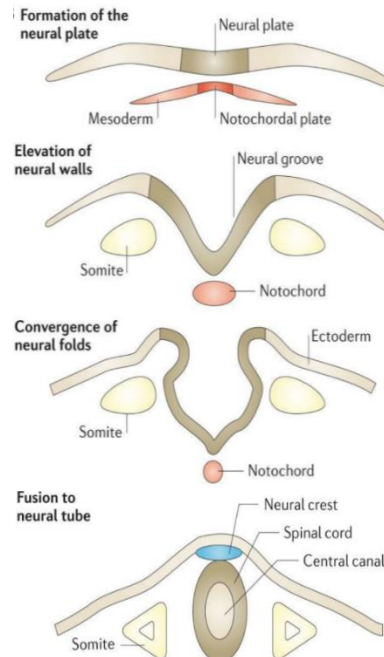


**Figure 2: Schematic diagram of neural tube closure in the developing mouse.** Some of the mesodermal cells will aggregate and form the notochord (Red) to give rise to neural plate and neural tube (Dark Green). Zone above the neural tube becomes neural crest cells (Blue). Modified with permission (16).

3) Prenatal brain neurogenesis and gliogenesis

The NSC and the progenitors go through neurogenesis to generate neurons throughout all regions of the neural tube, where they begin to construct spatiotemporal sensitive niche along the axes of body. This process is accompanied by gliogenesis that generate astrocytes and oligodendrocytes for support and myelination (17). Despite their distinct and diverse end functions by the end of differentiation process, some glial cells and neurons have been found to have same primary progenitor cells or NSC (18). These NSC exposed to cerebrospinal fluid (CSF) in the ventricle at the apical surface of ventricular zone (VZ) starts with symmetrical division to proliferate (2) (Figure 3). After building up thicker cell layer, the NSCs switch to neurogenesis by transforming into radial glial cells (RGCs) by downregulating epithelial features like tight junction, and upregulation of astroglial proteins such as Glutamate Aspartate Transporter (GLAST), Serum S100β and Brain lipid-binding Protein (BLBP) (2, 19-20). Unlike NSC, RGCs favor asymmetrical division that leads to fate-restricted progenitor with ability to give rise to neurons, oligodendrocyte progenitor cells (OPCs) and astrocytes (6,18, 21). Other than their potential to differentiate into various cell types, RGCs have been also known to provide their basal axons as scaffolding to guide neuron migration across the cerebral cortex, while their mitotically active nucleus stays at the VZ (22).
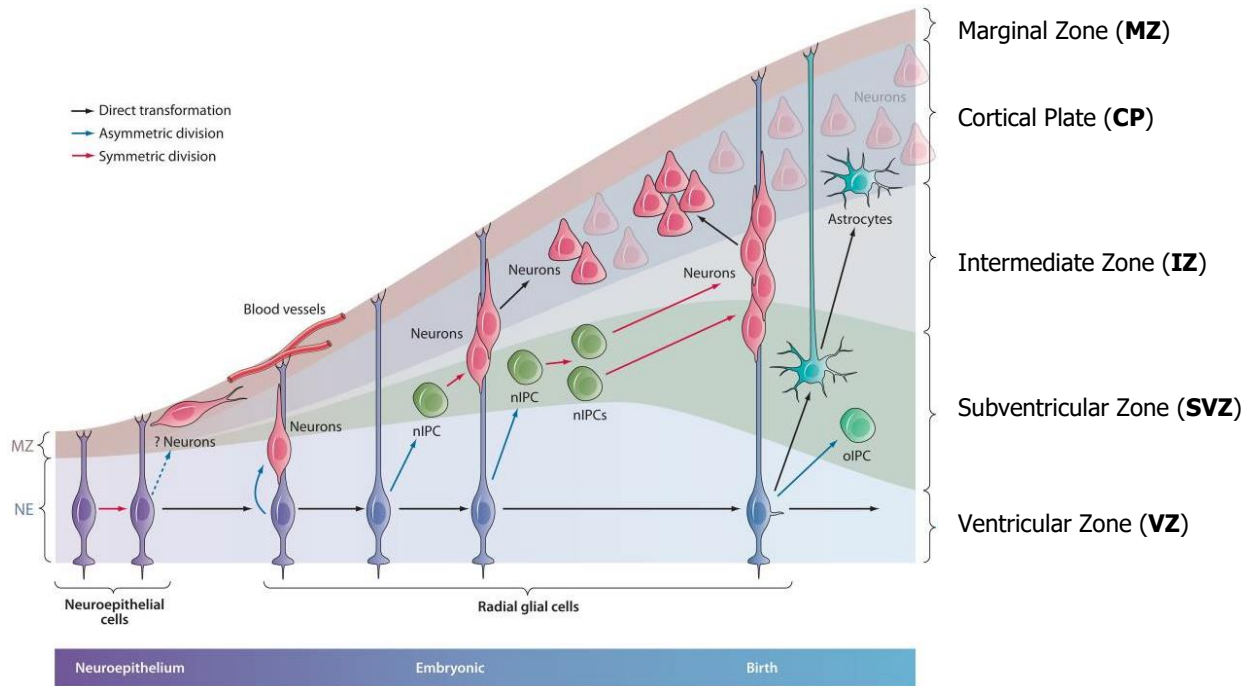
**Figure 3: Temporal development of the neocortex.** Neuroepithelial cells or NSCs go through symmetrical division initially, and then start taking form as radial glial cells (RGCs). RGCs can go through asymmetrical division to generate neurons, or oligodendrocyte progenitor cells (OPCs). At the end of embryonic development, RGCs detach from apical side of ventricle and become astrocytes. Modified with permission (18).

Corticogenesis, or generation of cerebral cortex is heavily active around E11-E19, but the cells can start losing epithelial makers and start expressing NSC marker Nestin as early as the time of neural tube closure at E9 (18, 20). Although the cells can have RGC like feature and start differentiating into neurons as early as E10, they can reach plateau for neurogenesis around E14-E15 (2, 20, 23-24) (Figure 4). During the corticogenesis, neurons and other cells will start forming transient multi-layered structure divided into several unique compartments on top of each other (24). Neurogenesis technically starts from ventricular zone (VZ), where the NSC with radial processes are exposed to cerebrospinal fluid filled with nutrients and morphogens, and will divide symmetrically to generate RGCs that will become precursor to actual neurons (6, 17-18, 22-25). Subventricular zone (SVZ) above VZ is created from NSC and RGC mitosis at the basal

surface of VZ and many cells in this layer are thought to undergo terminal symmetrical division

to produce migrating neurons (25). Above SVZ, intermediate zone (IZ) contains migrating cells

traveling via axons of RGCs or in tangential orientation, and axons that will eventually establish

white matter in the brain (25-26). Cortical plate (CP) and marginal zone (MZ) are the major

destinations for migratory cell terminal differentiation, with more newly differentiated neurons

staying in MZ above and push older neurons to CP in mouse brain (25, 27).
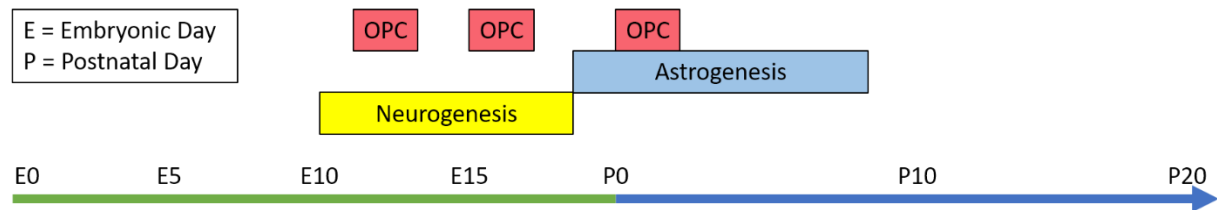


**Figure 4: Timeline for cellular process in the developing mouse brain.** Widely accepted
starting date for neurogenesis is around E10-E11 when the neural tube closes, and then peak and
persist through E14-E18. Astrogenesis starts around the end of neurogenesis and persist through
P7. OPC generation wave occurs at E12.5, E15.5, and P0 (2, 20, 23-25, 28).

After RGCs complete asymmetrical division to produce neurons during the neurogenesis

wave, they can either directly differentiate into astrocytes or produce intermediate cells that will

become astrocytes (28). While neurogenesis occurs as early as E10, the astrocyte differentiation

and maturation occur toward the end of neurogenic wave around E18 and last until

approximately postnatal day 7 (P7) (28) (Figure 4). The distribution and migration pattern of

neonatal astrocytes are still unknown due to lack of well targeted astrocyte marker (28-29).

Currently widely used markers like Glial Fibrillary Acidic Protein (GFAP) showed similar cell

distribution throughout the whole brain except the brain stem in both neonatal and adult rat brain,

suggesting that after glial cells are born in the VZ or SVZ, they might self-distribute themselves

and stay in the same location after migration (28). After birth, most postnatal astrocytes are

generated through local proliferation of already differentiated astrocytes that have migrated

throughout the whole brain shortly after birth in the VZ or SVZ (29). On the other hand,

oligodendrocyte progenitor cells (OPCs) comes in three major waves during prenatal period: 1)

on E12.5 in mice at the VZ of the medial ganglionic eminence (MGE), 2) on E15.5 at the lateral

ganglionic eminence (LGE), and 3) around birth at the cortex (21, 30) (Figure 4 and 5).
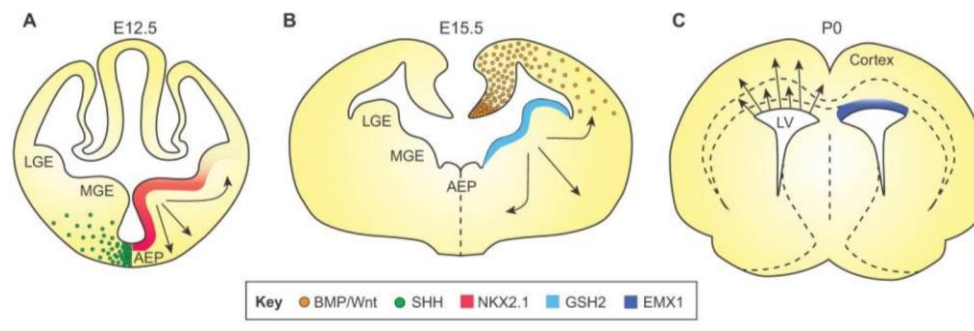


**Figure 5: Location of OPCs generation waves.** Coronal view of mouse forebrain indicating which area of VZ goes through different waves of OPCs generation during development. Modified with permission (30).

4) Postnatal brain neurogenesis and gliogenesis

Even though the neurogenesis and gliogenesis peak during embryonic development and post-

natal developmental period, neurogenesis and gliogenesis do persist through adulthood. Once

NSCs finish their set number of asymmetrical neurogenic divisions, they often undergo apoptosis

or terminal division, or enter senescence and decrease proliferation leading to decrease in NSC

numbers in post-embryonic animals, with only a few stem cells remaining in the adult brain (8).

After the birth, neurogenesis continues in area limited manner at the olfactory bulb (1)

subgranular zone (SGZ) of the denate gyrus within hippocampus and SVZ of lateral ventricle

that originated from embryonic radial glia (31) (Figure 6). In contrast to limited neurogenesis,

proliferation and migration of glial progenitors will continue postnatally, and will persist in adult

brain in a wide anatomical distribution and can differentiate in response to injury, and can

continue to proliferate as they migrate (1). OPCs will migrate toward the developing white

matter and undergo differentiation into mature oligodendrocytes through expanding its processes

and increase myelin protein expressing to begin myelination process (32).
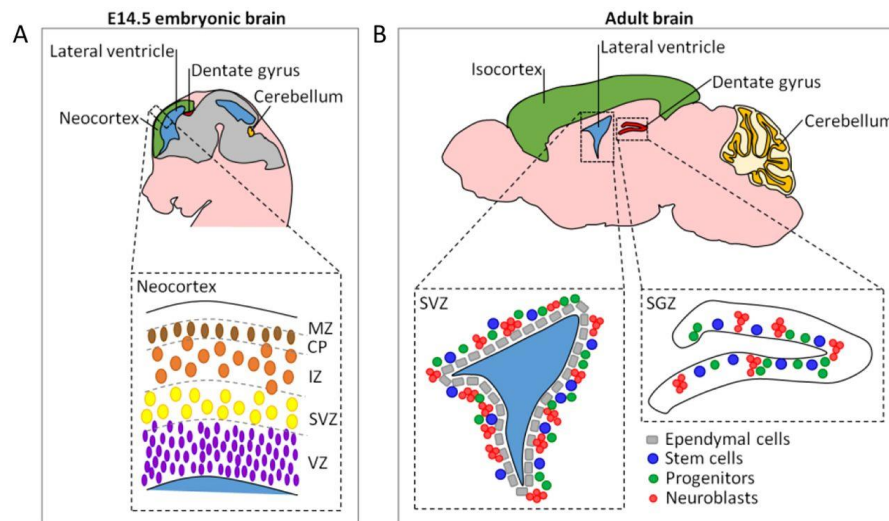


**Figure 6: Schematic diagram of the mouse embryonic and adult brain.**
(A) Sagittal view of E14.5 mouse brain. Main germinal zone in neocortex (green) are VZ and
SVZ near the ventricles (blue), IZ with migrating cells and axons, and CP encompassing post-
mitotic neurons. (B) Sagittal view of an adult mouse brain with neocortex developed into
isocortex (green). In adult brain, stem cells reside in subventricular zone (SVZ) of lateral
ventricle, and the sub-granular zone (SGZ) of the denate gyrus within the hippocampus.
Reproduced with permission (33).

5) *Spag17*

Sperm-associated antigen-17 protein (SPAG17) is the mammalian orthologue of PF6, a

protein present at the projection of C1 central pair microtubule in green algae, *chlamydomonas*

*reinhardtii* (34) (Figure 7). PF6 has been found to be vital component for assembly of a central

pair complex (CPC) and flagellar motility, confirmed by PF6 mutant's ineffective flagella and

missing C1a projection (35-37). It has been reported that C-terminal domain of PF6 are the

essential key player for flagellar motility and assembly of the C1a projection, while the N-

terminal half did more stabilization of the C1a complex members than assembly (37). Although the murine *Spag17* gene also encode a 250 kDa protein present in the CPC, the mammalian gene show greater complexity in expression patterns and functions (36) . In this context, other SPAG17 isoforms have been described in mammals that are cell/tissue specific. The full-length 250 kDa protein is found in testis and tissues with motile cilia like lung and brain, and a 97 kDa protein is present in testis and derived from an alternatively spliced variant (34, 36). The 97 kDa protein is cleaved to generate 72 kDa (N- terminal) and 28 kDa (C- terminal) fragments expressed in epididymal and ejaculated sperm (34, 36). These isoforms are believed to be important for motility of cilia and flagella, organelles known for having of axonemal central pair microtubule structure.
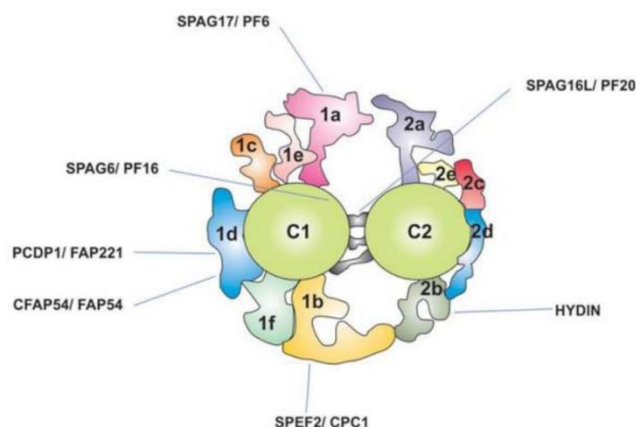


**Figure 7: Cross section of a Central Pair Complex.** SPAG17/PF6 (Pink) is projecting off of C1 complex. Reproduced with permission (36).

Dr. Teves' lab has been studying the *Spag17* gene for the last decade. Previous work done by Teves lab included first development of a knockout mouse model for this gene and report on how the gene plays role outside the tissues with motile cilia and flagella. The global *Spag17* KO they created showed phenotypes consistent with Primary Ciliary Dyskinesia (PCD) noted by neonatal respiratory distress and bronchiectasis secondary to disrupted alveolar epithelium, immotile nasal and tracheal cilia, reduced clearance of mucus, and lung fluid accumulation (38-39). In addition to that, magnetic resonance imaging (MRI) and histological examination confirmed that null-

mice had expanded cerebral ventricles consistent with hydrocephalus that are also associated with PCD, and neonatal demise within 12 hours of birth (38). Beside the classic phenotypes of PCD, the study of *Spag17* KO mice showed unexpected phenotypes incompatible with the role of the SPAG17 protein in motile cilia. Remarkably, KO mice show skeletal deformities, bone mineralization defects, and shorter primary cilia despite them not having CPC (35). These unexpected phenotypes called attention to new roles for *Spag17* in embryonic development and in tissues without motile cilia. In accordance with the finding in the murine model, a number of genome-wide association studies (GWAS) have reported an association between the human *SPAG17* locus and short stature (40-47). Moreover, a homozygous *SPAG17* mutation was found in a 7-year-old boy (48). The patient has multiple congenital anomalies including brain and bone deformities similar to those observed in the *Spag17* knockout mice, affecting cerebellum, lateral ventricles and corpus callosum. These compelling evidences, strongly suggest the involvement of SPAG17 in embryonic development, and pleiotropic functions outside motile cilia and flagella (35).

6) Hypothesis

In this study, we hypothesize that *Spag17* is crucial for cell differentiation during embryonic development of the brain, and the loss of *Spag17* will result in altered differentiation rate of neural stem cells, neurons, and the progenitor for glial cells like astrocytes and oligodendrocytes.

7) Specific Aims

In our first aim, our goal is to characterize the expression pattern and the location of *Spag17* throughout the development in CNS.

In our second aim, our goal is to determine how mice are affected by loss of the *Spag17* gene in the context of neural cell differentiating into either neuron or glial cells.

Chapter 2: Materials and Methods

1)  Animal model

All experimental protocols involving animal use were performed in accordance with the National Research Council's Guide for the Care and Use of Laboratory Animals, and protocol AM10297 approved by the Virginia Commonwealth University Institutional Animal Care and Use Committee. All efforts were made to minimize the potential for animal pain and stress.

*Spag17/CMV-Cre Knockout*

In order to generate global *Spag17* KO mice, embryonic stem (ES) cells were obtained from the Knockout Mouse Program (KOMP) at the Jackson Laboratory (Davis, CA). First, the chimeric male mice were generated using embryonic stem cell. The resulting chimeric males with LoxP-Flippase recognition site (FRT) upstream of target exon 5, were bred to C57BL/6NJ WT females. Their heterozygous offspring were then crossed to 129S4/SvJaeSorGt(ROSA)26Sor$^{tm1(FLP1)Dym}$/J (stock number: 003946) to introduce flippase (FLP) recombinase and remove section between two FRT sites. After that, *Spag17* mice with exon 5 between two LoxP sites, or floxed site were mated with *Cytomegalovirus-Cre* (*CMV-Cre*) mice (B6.C-Tg(CMV-Cre)1Cgn/J, stock number: 006054). These mice with C57BL/6J background introduced Cre recombinase to remove exon 5 between LoxP sites to produce heterozygous *Spag17/CMV-Cre* mice (Figure 8). The heterozygous male and female *Spag17/CMV-Cre* mice were then mated to give birth to homozygous *Spag17/CMV-Cre* knockout mice at near expected Mendelian ratios.

The global deletion of *Spag17* resulted in either embryonic lethality or lethality within 12 hours of birth after respiratory distress (38). All mice were bred in our animal colony to obtain mice at each age examined at embryonic age 15.5 and postnatal day 0 (P0). The day with plugs

were considered as the day 0.5 and P0 the day of birth. These *Spag17/CMV-Cre* mice were

sacrificed at E15.5 and P0 for slide sectioning and primary cell culture, and were stained with

Nestin, Tuj1, and NeuN primary antibodies. For immunohistochemistry, the slide sections from

six different animals were tested and quantification were done two to three times on E15.5. For

P0 mice, the slide sections from three different animals used for testing and quantification of

IHC done with primary antibodies against Nestin, Tuj1, and NeuN.

*Spag17/Sox2-Cre knockout*

The *Spag17/Sox2-Cre* knockout mice were obtained from the Knockout Mouse Program

(KOMP) at the Jackson Laboratory (Stock Number: 026485). The *Spag17/Sox2-Cre* mice were

generated using the same vector than *Spag17/CMV-Cre* mice. Unlike the *Spag17/CMV-Cre* mice

that were crossed to mice with FLP recombinase and then Cre recombinase, *Spag17/Sox2-Cre*

mice were bred to only *Sox2-Cre* mice to remove the exon 5 between LoxP sites (Figure 8).

Therefore, heterozygous *Spag17/Sox2-Cre* mice retain the LacZ reporter upstream of exon 5 site,

allowing *Spag17* gene expression monitoring with beta-galactosidase assay.  For β -gal, embryos

were sacrificed and collected at the age of E11, E11.5, E14.5, E15.5 and E17.5, at least twice for

each time point.
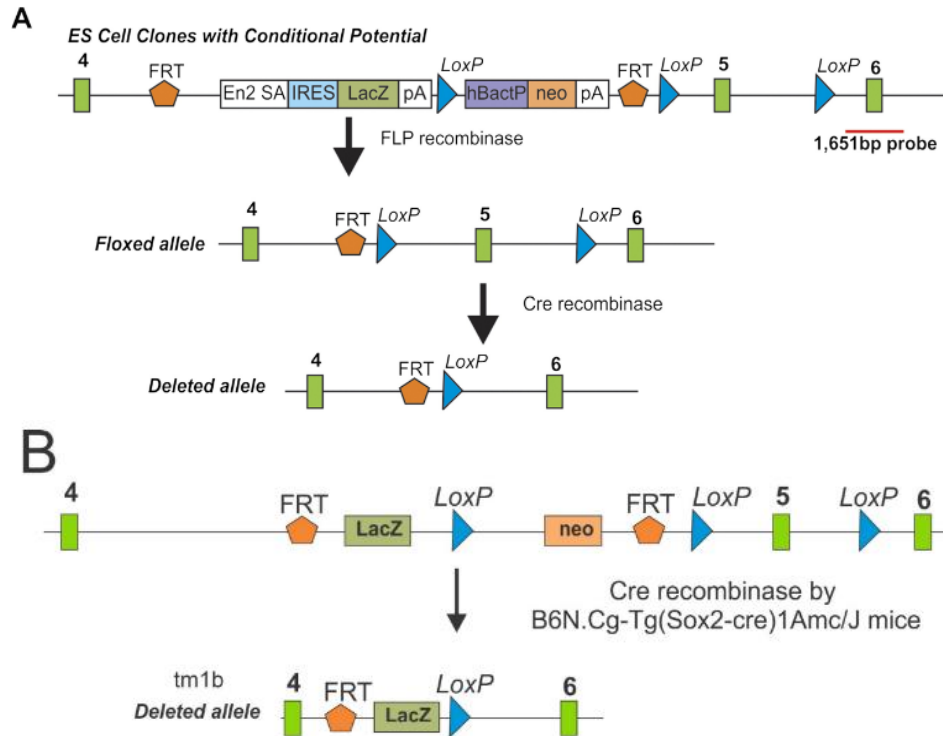
**Figure 8. Strategy for disruption of the *Spag17* gene**. (A) Schematic representation of CMV-Cre mice FLP-FRT and Cre-Lox recombination for exon 5 deletion, (B) Schematic representation of tm1b mice cre-recombination for exon 5 deletion. Reprinted with permission of the American Thoracic Society. (38, 49)

*Genotyping*

First, the mouse DNA was isolated by incubating tissue in lysis buffer containing 1M pH 8 Tris-HCL, 5M NaCl, 10% SDS, 0.5M EDTA pH8, 10 mg/mL proteinase K, and diH2O. After initial digestion overnight in 55°C incubator, DNA was precipitated using isopropanol and dissolved in Tris-EDTA pH 7.4 in 55°C incubator for 2 hours. Dissolved DNA was used for genotyping by PCR. For *Spag17/CMV-Cre* mice, the primer sequence used were forward: 5'-GCACTCCAAAATTGGGCTAA-3' and reverse: 5'-GAGTGAGCAACTTTCCTCAGGAG-3' primers were used. For *Spag17/Sox2-Cre* mice, the set of primers used were forward 5'-CTGTCTTGATGAGAATGTAATG-3' and forward 5'-CCCTGAACCTGAAACATAAA-3', and reverse 5'-GAGTGAGCAACTTTCCTCAGGAG-3'.

2) Beta-galactosidase staining

   To visualize the location of the *Spag17* gene expression, heterozygous male and female

*Spag17/Sox2-Cre* mice embryos were stained with whole mount β-Galactosidase. After the

embryos were removed from mother, they were washed with PBS to remove blood. The embryos

were then fixed in 1X fixation buffer with 20% formaldehyde and 2% glutaraldehyde in PBS for

1-4 hours depending on embryonic age and size. After fixation, they were quickly rinsed with

PBS and incubated in PBS for 30 minutes. The embryos were then kept in the staining solution

with 200 mM $MgCl_2$, 400 mM potassium ferricyanide, 400 mM potassium ferrocyanide, and 20

mg/mL of X-gal in 1X PBS overnight in the dark at 37°C. To avoid endogenous β-Gal activity,

pH was kept around 7.5 to 8.5. For older embryos between E13.5-15.5, the embryos were

permeabilized with 0.02% NP-40 detergent added to the staining solution mentioned above. The

stained embryos were rinsed with PBS next day and were then incubated in PBS for 30 minutes.

Following the fixation and PBS rinsing, embryos that are E12.5 or older were dehydrated via

immersion in increasing concentration of ethanol in glass vials for 30 minutes each and overnight

in 100% ethanol (EtOH). After overnight incubation, the embryos were re-incubated in fresh

100% EtOH for another 30 minutes and then transferred to 10 mL1:1 benzyl benzoate and

benzyl alcohol for clearing.

3) Immunohistochemistry (IHC)

   For postnatal IHC sample collection, mice were anesthetized using isoflurane and then

decapitated. For embryo samples, their gestational mother was sacrificed using isoflurane and

then extracted through surgical incision. The brains were fixed in 10% formalin for 3 days in 4°C.

After paraffin embedding at the Virginia Commonwealth University Massey Cancer Center

Cancer Mouse Models core, each head was then sagittal sectioned with microtome at 15 μm thickness and placed on charged-slides in the water bath.

*Immunohistochemical staining*

For staining, the sections of samples were obtained from identical regions of the wild-type and knockout brains that were selected based on structural and anatomical landmarks. Those selected slides were incubated in 55°C for 1 hour, and then deparaffinized with xylene, and then rehydrated through decreasing concentration of ethanol. The slides were then treated with 3% $H_2O_2$ for 30 min to remove endogenous peroxidase. Antigen retrieval was performed in citrate buffer at 95°C for 20 min. After washing several times in PBS, slides were blocked with 10% goat serum, 0.2% triton X-100 buffer in PBS for 1 hour in room temperature. Following the blocking, the slides were incubated overnight with primary antibodies against Nestin (catalog #14-5843-82, Invitrogen), Tuj1 (catalog #T8578, Sigma-Aldrich), and NeuN (catalog #MAB377, Millipore) diluted in blocking buffer at 4°C. After washing slides with PBS thrice for five minutes each, the slides were incubated in biotinylated species-specific secondary antibody (Vector laboratories, Burlingame, CA) diluted in blocking buffer for 1 hour in room temperature. Following the incubation, the slides were washed with PBS thrice for 5 minutes each to remove excess antibody. The slides were then incubated with Vectastain Avidin-Biotin-Complex (ABC) reagent for 30 minutes in room temperature. The slides were again washed with PBS thrice for 5 minutes. The staining was developed with ImmPACT Diaminobenzidine (DAB) for 2-10 minutes (depending of the primary antibody used) and were rinsed with cold tap water to stop the reaction. WT and KO samples were processed in parallel to ensure the same conditions for these samples. The stained slides were dehydrated using increasing concentration of ethanol and xylene and were mounted using Vectastain mounting media.

4) Cell culture and immunofluorescence (IF)

For neuronal cell culture, E14.5 WT and *Spag17/CMV-Cre* KO mouse brains were collected to observe cell differentiation *in vitro*. After pregnant mouse was anesthetized using isoflurane and cervical dislocated, uterus with embryos were surgically removed and checked for age specific characteristic. Removed uterus was washed in cold sterile PBS twice, and embryos were removed from amniotic sac using curved forceps. Those individual embryos were transferred to separate petri dishes, emerged in PBS while head was decapitated. After removal of meninges with forceps, the entire brain was transferred to DMEM with antibiotic to be dissected with scissor. Subsequently, minced brain fragments were transferred to conical tube with DMEM, antibiotic and trypsin to be incubated in 37° for 30 min with occasional gentle agitation. The tubes were then centrifuged, resuspended in media with DMEM, FBS and antibiotic, and strained through 100 μm mesh strainers. After one more centrifuge and re-suspension in cell media, they were seeded onto 8 well chamber slides coated with gelatin 0.1%. Media was changed every 48 hours until the cell culture were confluent by 80-90% and ready for fixation and IF.

For IF, the cell culture within chamber slides were washed with PBS twice, and were incubated in 10% formalin for 1 hour in room temperature (RT). After 1 hour in formalin and PBS washing for 10 minutes thrice, the cells were incubated with blocking buffer containing 10% goat serum, 3% BSA, and 0.2% Triton X-100 for 1 hour in RT. The cells were then incubated with blocking buffer diluting the primary antibodies against Tuj1 at 4°C overnight. Next day, the cells were washed with PBS for 10 minutes thrice, and were incubated with secondary antibodies labeled with Alexa Fluor 594. After last PBS washing for 10 minutes thrice, the well divider for chamber slides were removed and the slides were mounted with DAPI mounting media.

5) Data analysis

The representative images were obtained from independent experiments, repeated at least in duplicate. The slide images were viewed and captured with Vectra Polaris Automated Quantitative Pathology imaging system (Perkin Elmer), Phenochart (Perkin Elmer), Olympus BH-2 microscope (Olympus, Center Valley, PA), LSM 710 (Zeiss), and Discovery V20 Stereo zoom fluorescence stereoscope (Zeiss). The quantification and analysis of stained slides were done using image analysis software (cellSense, Olympus). Relative differences in staining at the region of interest were measured by highlighting specific stained areas with red overlay. Data were quantified as area stained ($\mu m^2$) and presented as relative percentage $\pm$ SEM. The differences between two groups were analyzed with unpaired, two-tailed Student's t-test. p-value of less than 0.05 was considered as statistically significant for this study. Statistical analysis was performed using GraphPad QuickCalcs software (https://www.graphpad.com/quickcalcs/ttest1/).

Chapter 3: Results

1) *Spag17* is expressed in several tissues throughout the embryonic development

Expression of *Spag17* in the areas with known presence of motile cilia like ependymal cells lining the ventricles of brain, respiratory epithelial cells as well as in the sperm flagella were already known (38). However, there were still questions regarding the expression of *Spag17* in the developing brain and tissues without motile cilia (35).

To outline the spatiotemporal expression of *Spag17*, β-galactosidase (β-Gal) assay was performed on heterozygous *Spag17/Sox2-Cre* embryos consisting of a LacZ reporter linked to the *Spag17* gene. The embryos were collected from pregnant females at different embryonic stages (E11.0 to E17.5) and the appearance of blue staining was considered a marker for expression of *Spag17*.

β-Gal blue staining was observed in embryonic day 11 at the neural tube, a structure that will later become spinal cord and brain (Figure 9A). Few hours later when embryo become E11.5, the expression of *Spag17* was expanded to rhombic lip and still present in neural tube at the same time (Figure 9B). As previously discussed, rhombic lip can further segment into smaller region called rhombomeres, and most anterior hindbrain segment rhombomere 1 (R1) will become the primary source of cerebellar granule cell precursors, which will constitute more than half of the adult neuron cell population (14-15). When the embryos reach E14.5-E15.5, *Spag17* expression was present at the frontal cortex, lateral ventricle and intensified even further at the rhombic lip (Figure 9C). At E17.5, *Spag17* was intensely visualized at the cerebral cortex, corpus callosum between cortices, midbrain, cerebellum, and still present throughout the neural tube (Figure 9D).
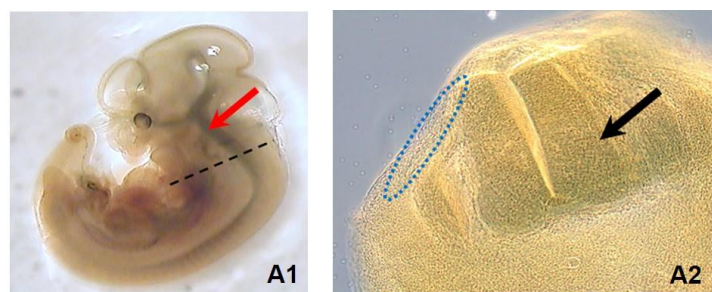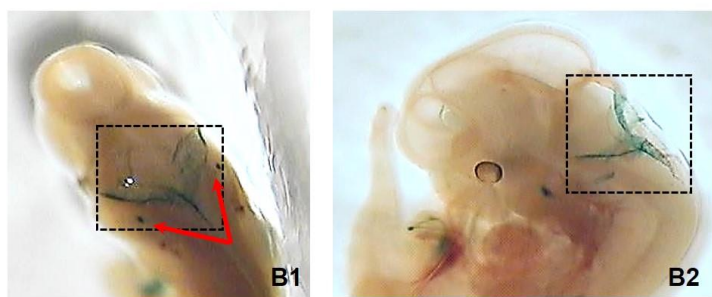
**Figure 9. β-galactosidase assay showing expression of *Spag17* at different embryonic stages.**
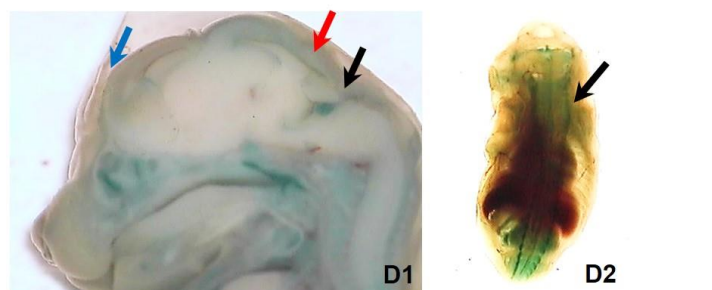
**A1)** Lateral view of E11.0 embryo with β-Gal staining at the neural tube (Red). **A2)** Transverse section at black dotted line on A1. The staining is visible at the neural tube (Black) as well as neural crest cell within the dotted circle (Blue).

**B1)** Dorsal and **B2)** lateral view of E11.5 embryo with β-Gal staining at the rhombic lip (Black) and optic vesicle indicated by arrow (Red).
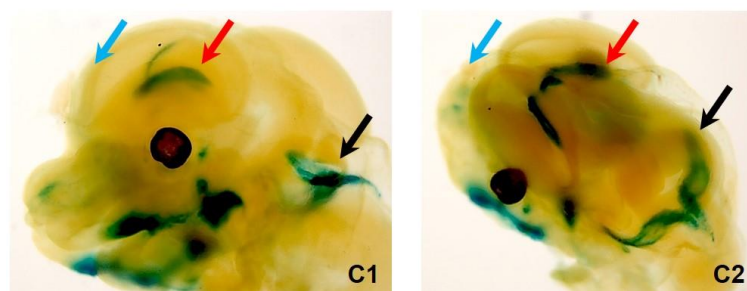
**C1)** Lateral and **C2)** Cranial view of E14.5-E15.5 embryo head with *Spag17* expression at frontal cortex (Blue), lateral ventricle (Red) and rhombic lip (Black).

**D1)** Lateral view of E17.5 embryo head with β-Gal staining at the frontal cortex (Blue), midbrain (Red), and cerebellum (Black). **D2)** dorsal view of the of body with expression at spinal cord (Black). **D3)** frontal view of head with *Spag17* expression across the corpus callosum (Black) **D4)** Dorsal view of head with expression at the cerebellum (Black).
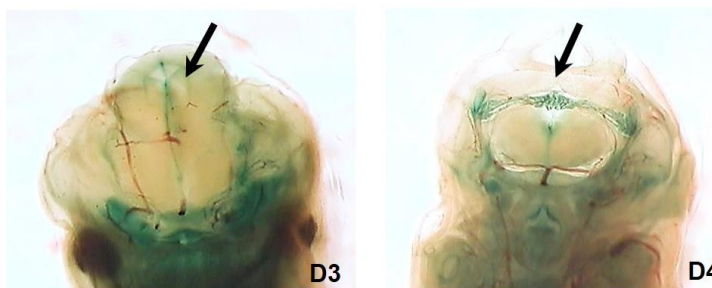
After β-Gal assay was used to characterize *Spag17* expression in the embryo, IHC was performed on P0 WT mouse brain to profile expression of SPAG17 protein in post-natal brain. SPAG17 was observed throughout the brain, but especially at the cerebral cortex, hippocampus, olfactory bulb, midbrain, and cerebellum, consistent with areas visualized in β-Gal (Figure 10).
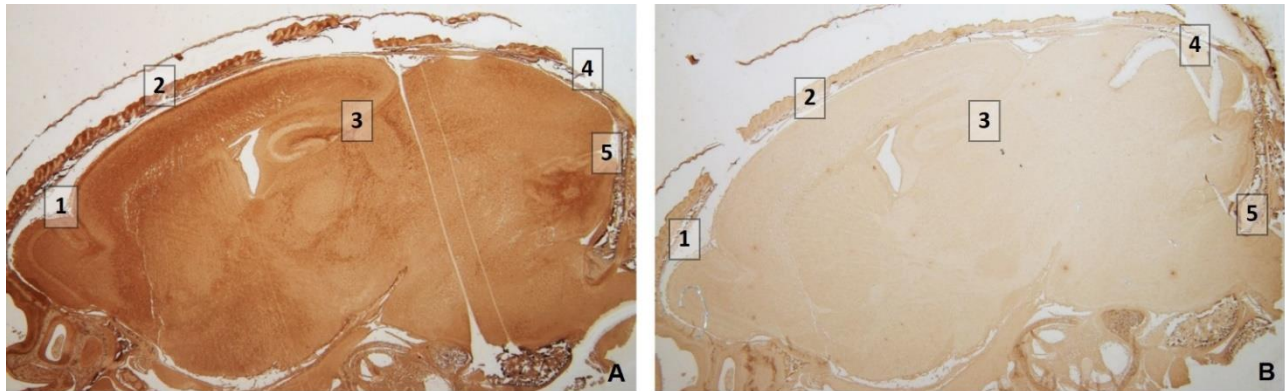


**Figure 10. P0 *Spag17* WT brain stained with SPAG17 antibody** (A) Sagittal section of P0 WT mouse brain stained with 1° ab against SPAG17. (B) Sagittal section of P0 WT brain negative control. Strong protein expressions are seen at 1-Olfactory bulb, 2-Cerebral Cortex, 3-Hippocampus, 4-Midbrain, and 5-Cerebellum on (A).

2) *Spag17* mutants exhibit delay in neuronal cell differentiation and maturation

IHC was performed in WT and *Spag17/CMV-Cre* knockout E15.5 embryos and P0 neonates to determine whether *Spag17* may be important for cell differentiation and maturation. Both WT and KO brain samples were sagitally sectioned and were stained with primary antibodies tagging proteins expressed at the different stages of neuronal maturation. The sections were selected based upon the presence of anatomical landmarks and similar sectioning depth.

*Neural Stem Cell and Radial Glial Cell*

Nestin is a class VI intermediate filament protein uniquely expressed in neural stem cells and radial glial cells, and are known to be involved in cytoskeleton developmental remodeling regulation (50). They initially appear in NSC when they start losing epithelial characteristic after neural tube closing at E11, and persist until they differentiate into other cell types like neuron or glial cells (2, 19). As previously discussed, NSC are expected to be present at the VZ and SVZ apical to the lateral ventricle. In P0, they are expected to be near SVZ and dentate gyrus of hippocampus. Nestin was used in our experiments to detect NSC and RGCs to see if they are expressed differently in WT and KO at the same stage during the development. Also, it was tested on P0 to see if KO will have same pattern persisting after the birth.

Throughout two to three independent experiments done on E15.5 embryo brains, the most significant differences between WT and *Spag17/CMV-Cre* KO were observed at cerebral cortex and R1, with KO brain showing 2.2 times more Nestin positive area than WT at the cerebral cortex, and 1.5 times more at the R1 (Figure 11-12). This suggests that in the absence of *Spag17*, NSC and RGCs at the cerebral cortex and R1 are affected, consistent with E15.5 β-Gal staining showing presence of *Spag17* gene at the lateral ventricle, cerebral cortex and rhombic lip (Figure 9). This relative Nestin positive area differences between WT and KO trend persist in P0 cerebral cortex and rhombomere 1 (not shown), as well as hippocampus. In the hippocampus, both WT and KO had strong positive Nestin signal at the dentate gyrus, a known neurogenic area, but KO had overall 2.5-fold of positive Nestin signal in KO (Figure 13). Similar to E15.5, P0 Nestin staining at the hippocampus is supported by P0 WT IHC showing strong presence of SPAG17 at the same area (Figure 10).

**Figure 11. E15.5 Cortex stained with Nestin.** Representative sections of E15.5 Cortex from WT (Top) and KO (Bottom) immunostained with NSC and RGC marker Nestin. The region of interest (ROI) and the specific antigen staining within the area has been highlighted and overlayed with red using cellSens software. With WT as 1, KO had about 2.2-fold of positive signal within same area of interest. Each data point was compared using unpaired t-test. Data are means +/- SEM of experiments. *P<0.05. n=3
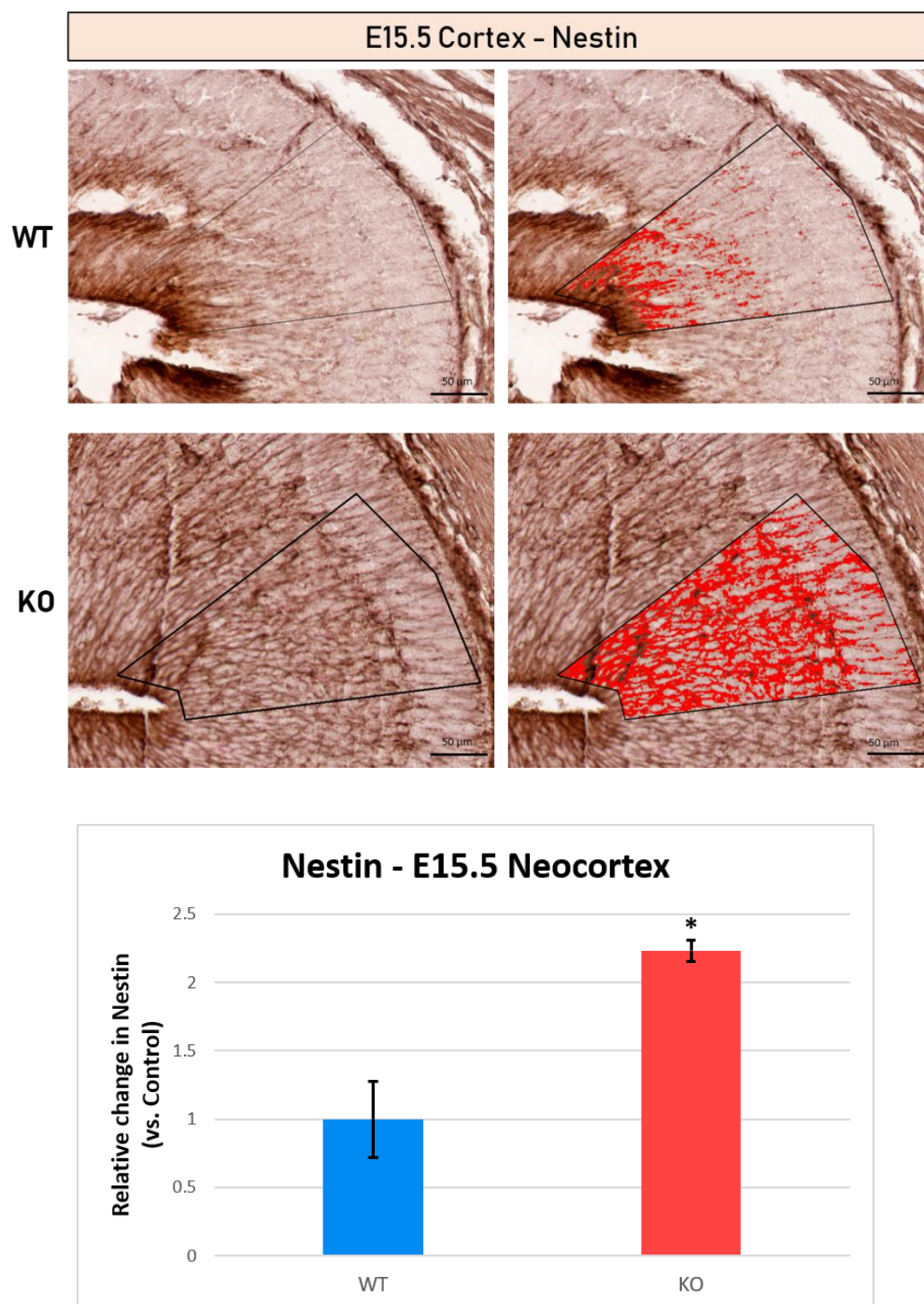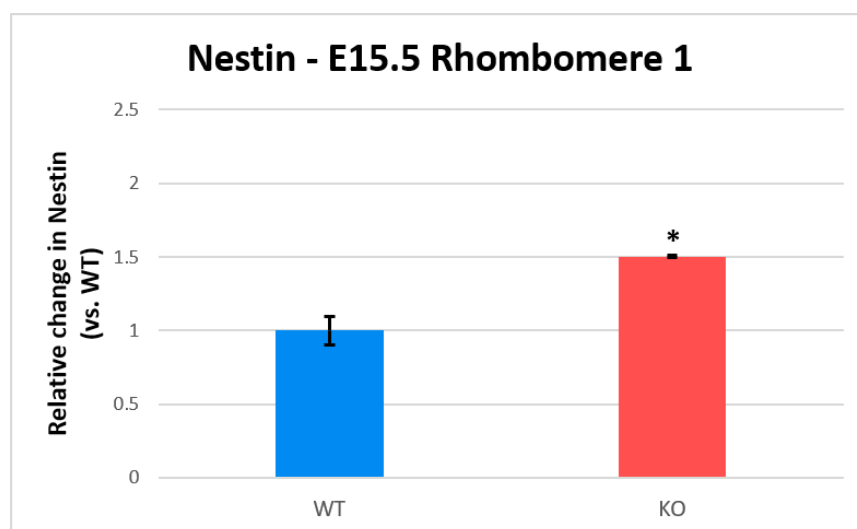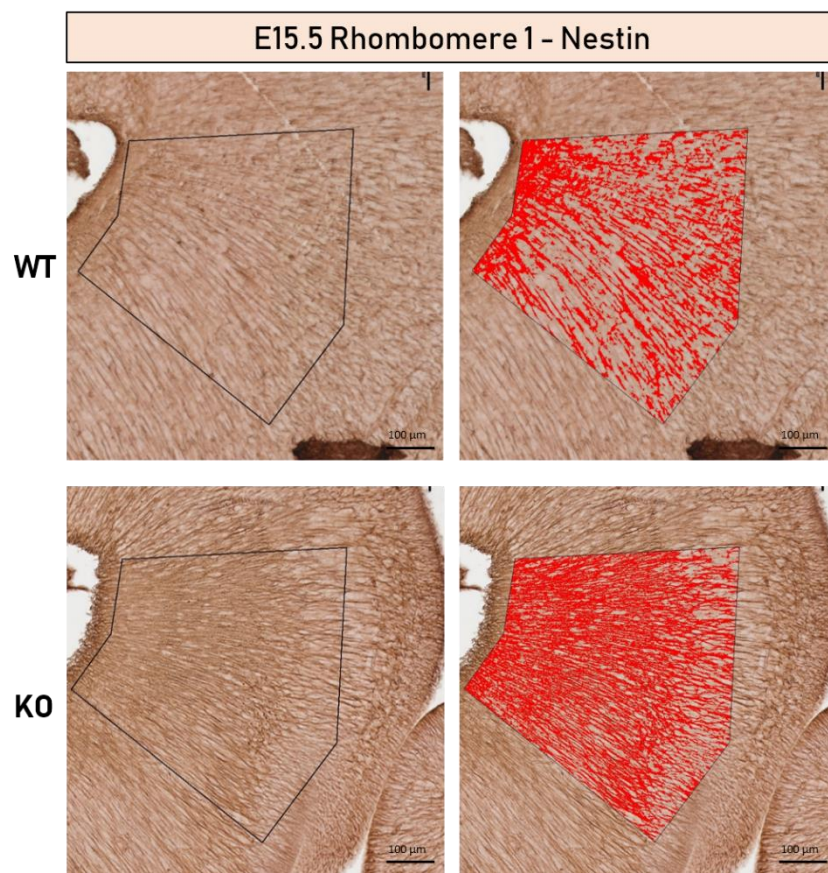
**Figure 12. E15.5 Rhombomere 1 (R1) area stained with Nestin.** Representative sections of E15.5 R1 from WT (Top) and KO (Bottom) immunostained with NSC and RGC marker Nestin. The region of interest (ROI) and the specific antigen staining within the area has been highlighted and overlayed with red using cellSens software. With WT as 1, KO had about 1.5-fold of positive signal within same area of interest. Each data point was compared using unpaired t-test. Data are means +/- SEM of experiments. *P<0.05. n=2

**Figure 13. P0 Hippocampus area stained with Nestin**. Representative sections of P0 hippocampus from WT (Top) and KO (Bottom) immunostained with NSC and RGC marker Nestin. The region of interest (ROI) and the specific antigen staining within the area has been highlighted and overlayed with red using cellSens software. With WT as 1, KO had about 2.5-fold of positive signal within same area of interest. Each data point was compared using unpaired t-test. Data are means +/- SEM of experiments performed in triplicate. *P<0.05. n=3
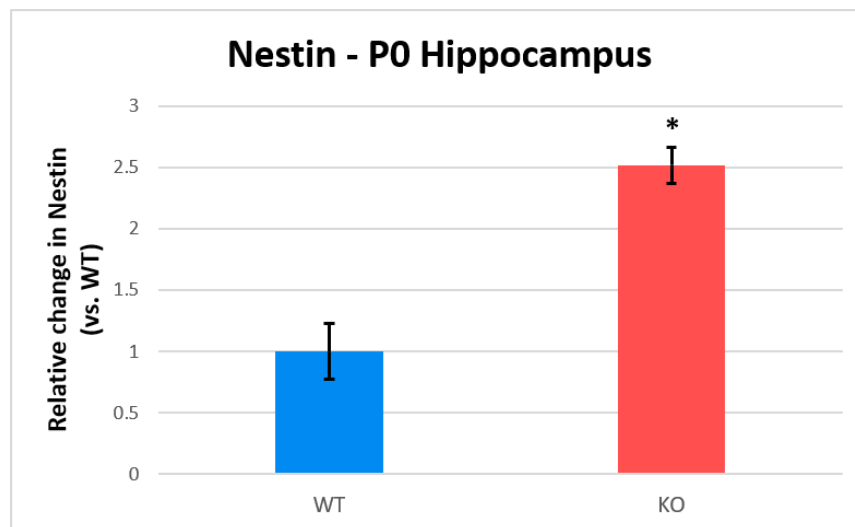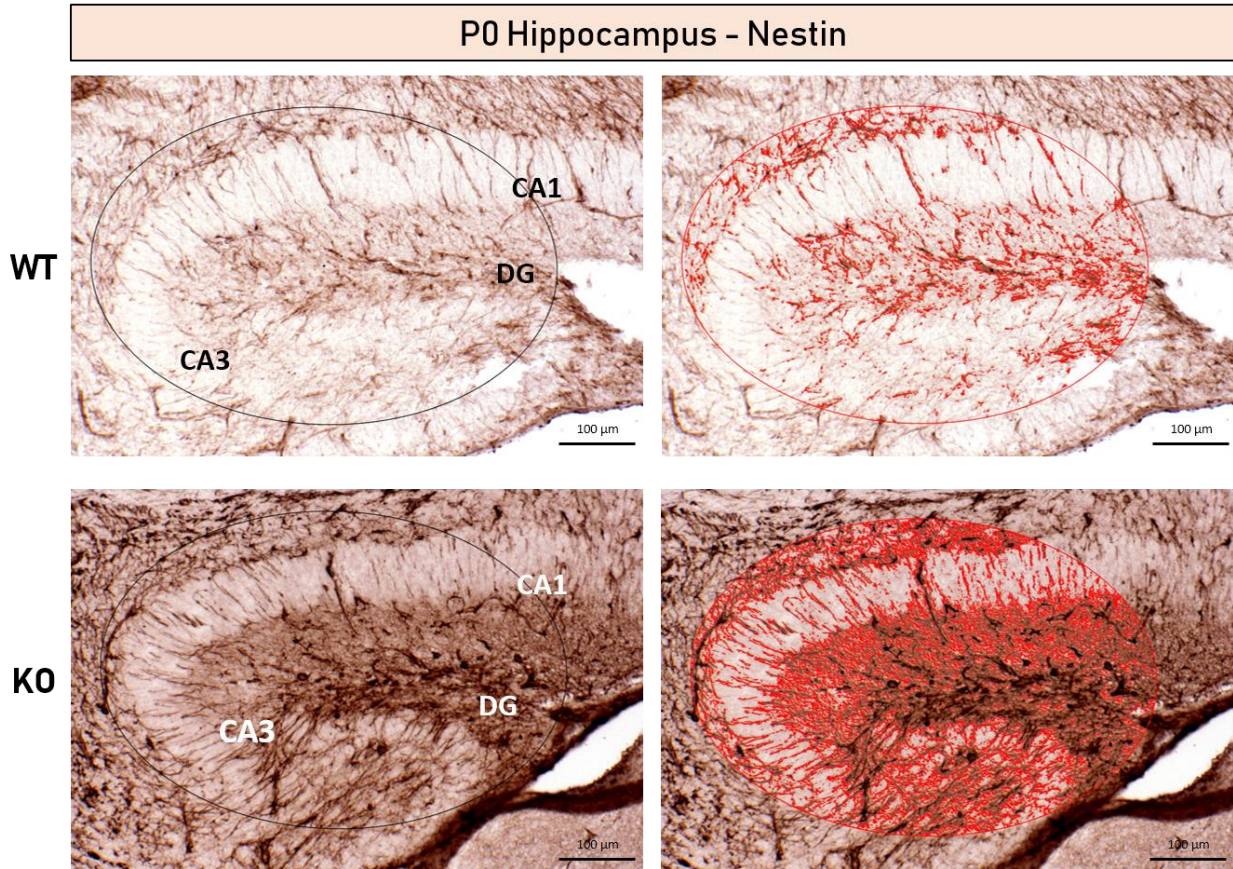
*Immature Neurons*

Tuj1, or Neuron-Specific Class III beta-tubulin, is expressed in the cytoplasm and axons of immature neurons that are migrating from SVZ to CP. Their immunoreactivity first appears at the cerebral cortex around E13-E14 at the CP near the basal surface of the cortex, and increases even further in the area between VZ and SVZ after E14 (23). Tuj1 is known to be expressed in immature neurons who are either very early, during or immediately after mitotic cycle (23). However, they are even more unique subset of population different from other post-mitotic migrating neurons by migrating in non-radial orientation without using radial glial processes (23). Other than expressing Tuj1, immature neurons are distinctive from mature neurons in morphology with less complex dendritic tress and reduced spine density (51). Tuj1 staining was used to highlight newly generated post-mitotic cells to examine what steps might be heavily affected by *Spag17* KO.

Tuj1 positive signals were detected on the E15.5 cerebral cortex using IHC. Figure 14 shows normal distribution of immature Tuj1 positive neurons mostly distributed at the SVZ, IZ, and CP, with very little number of cells at the VZ indicating that the cells were normally migrating towards the CP. However, *Spag17/CMV-Cre* KO animals showed lightly differences in the pattern of expression of Tuj1. It appears that KO brains may have more Tuj1 positive cells at the VZ and SVZ compared to WT animals of same age group. Although, KO had 1.3-fold of positive Tuj1 signal than WT, quantification of the image using the IHC analysis program cellSens did not show statistically significant different between WT and KO (Figure 14). This might be due to lower number of samples analyzed and increased variation between animals. For Tuj1, IHC done on some of the E15.5 and P0 were not eligible for quantification due to the lack of tissues with matching anatomical features and area.
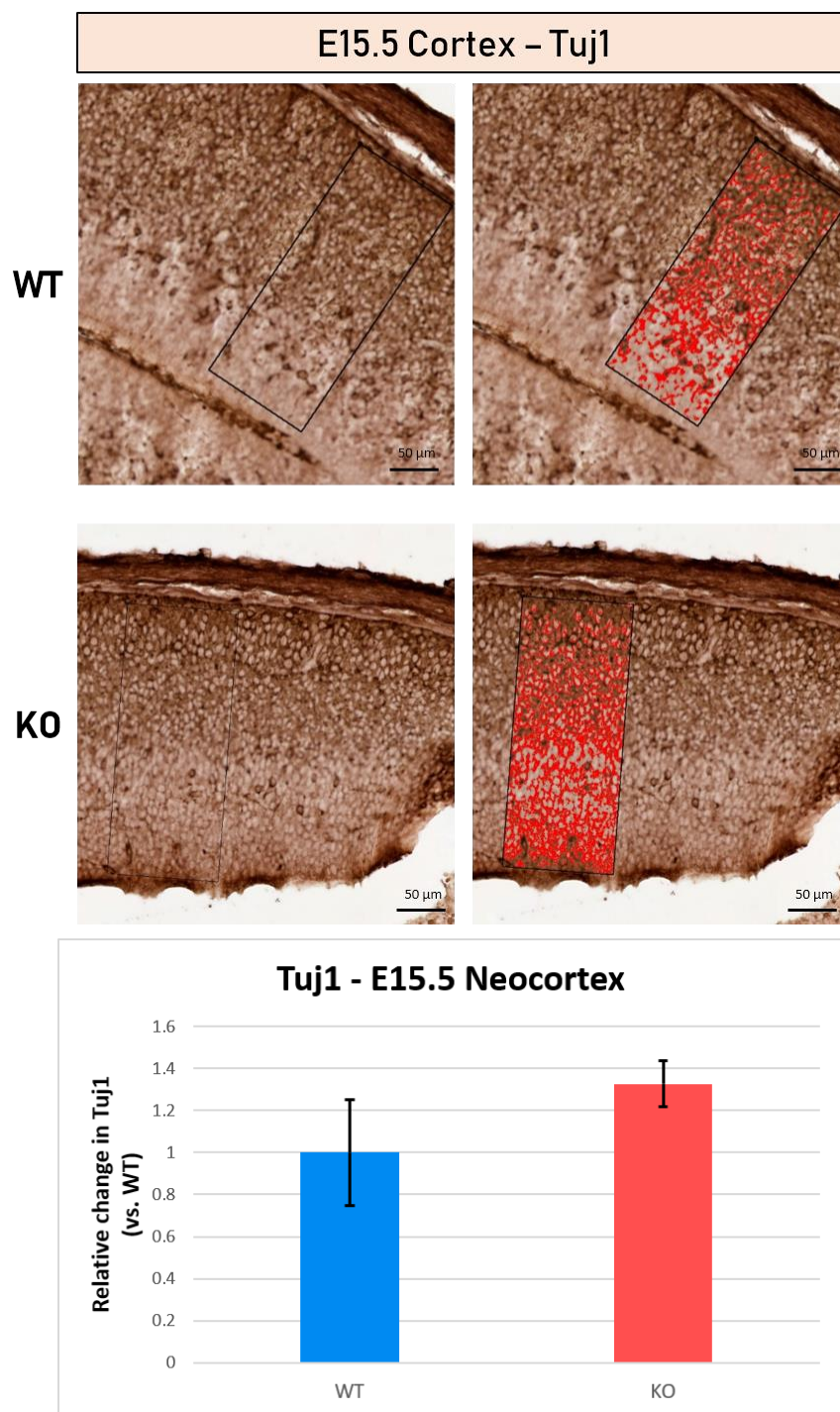
**Figure 14. E15.5 Cortex stained with Tuj1.** Representative sections of E15.5 Cortex from WT (Top) and KO (Bottom) immunostained with immature neuron marker Tuj1. The region of interest (ROI) and the specific antigen staining within the area has been highlighted and overlayed with red using cellSens software. With WT as 1, KO had about 1.3-fold of positive signal within same area of interest. Each data point was compared using unpaired t-test. Data are means +/- SEM of experiments performed in triplicate. *P<0.05. n=3

Later, we collected neuronal cells from E14.5 WT and *Spag17/CMV-Cre* KO brains and

proliferated them to study cell differentiation and maturation *ex vivo*. The expression of

immature neuron cell marker Tuj1 on neuronal cell culture of WT and *Spag17* KO brains were

evaluated under the confocal fluorescence microscope after IF. Figure 15 shows *Spag17* KO

having more Tuj1 positive signals than WT cells. This is similar to what was observed in the

IHC with 1.3-fold increased signal of Tuj1-positive cells in the cortex, suggesting that *Spag17*

KO brains have more immature neurons than WT of same age group.
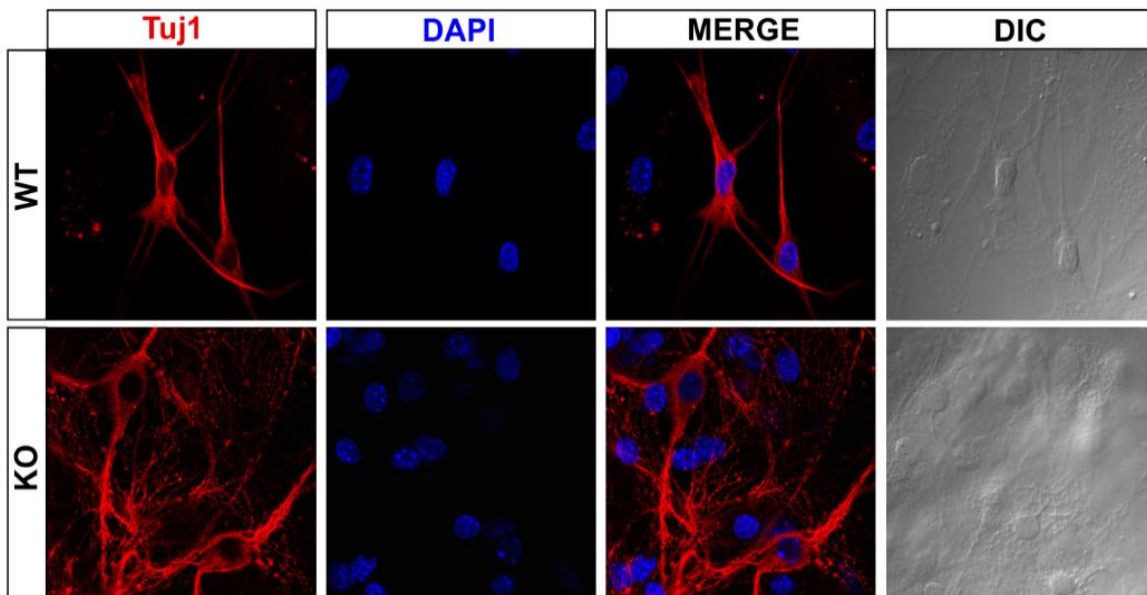


**Figure 15. Immunofluorescence evaluation of Tuj1 expression in cultured neurons.**
Representative images of immature neurons collected from E14.5 WT and *Spag17* KO
brains. WT (Top) and KO (Bottom) cells were immunostained with Anti-Tuj1 antibody
(red). Differences in area with positive signal and morphology were observed under
confocal microscope.

*Mature Neurons*

As immature neurons expressing Tuj1 start to exit from the cell cycle and initiate terminal differentiation near the CP, the cells will downregulate Tuj1 and will upregulate mature neuron-specific nuclear protein called Neuronal Nuclei or NeuN (52). NeuN is known for their high specificity to nervous tissue and does not detect immature neural progenitor cells as long as they are completely out of cell cycle (53). NeuN will be observed in most neuronal cell types within the brain except cerebellar Purkinje cells, olfactory bulb mitral cells, and retinal photoreceptor cells (52-53).

In our three independent experiments done on E15.5 embryo brains, NeuN positive cells were detected on E15.5 cerebral cortex, with KO having 60% less NeuN expression than WT of same age group (Figure 16). This suggests that loss of *Spag17* may be associated with defects in the maturation of neurons. Similar to Tuj1, NeuN IHC done on some of the E15.5 and P0 were not eligible for quantification due to the lack of tissues with matching anatomical features and area.
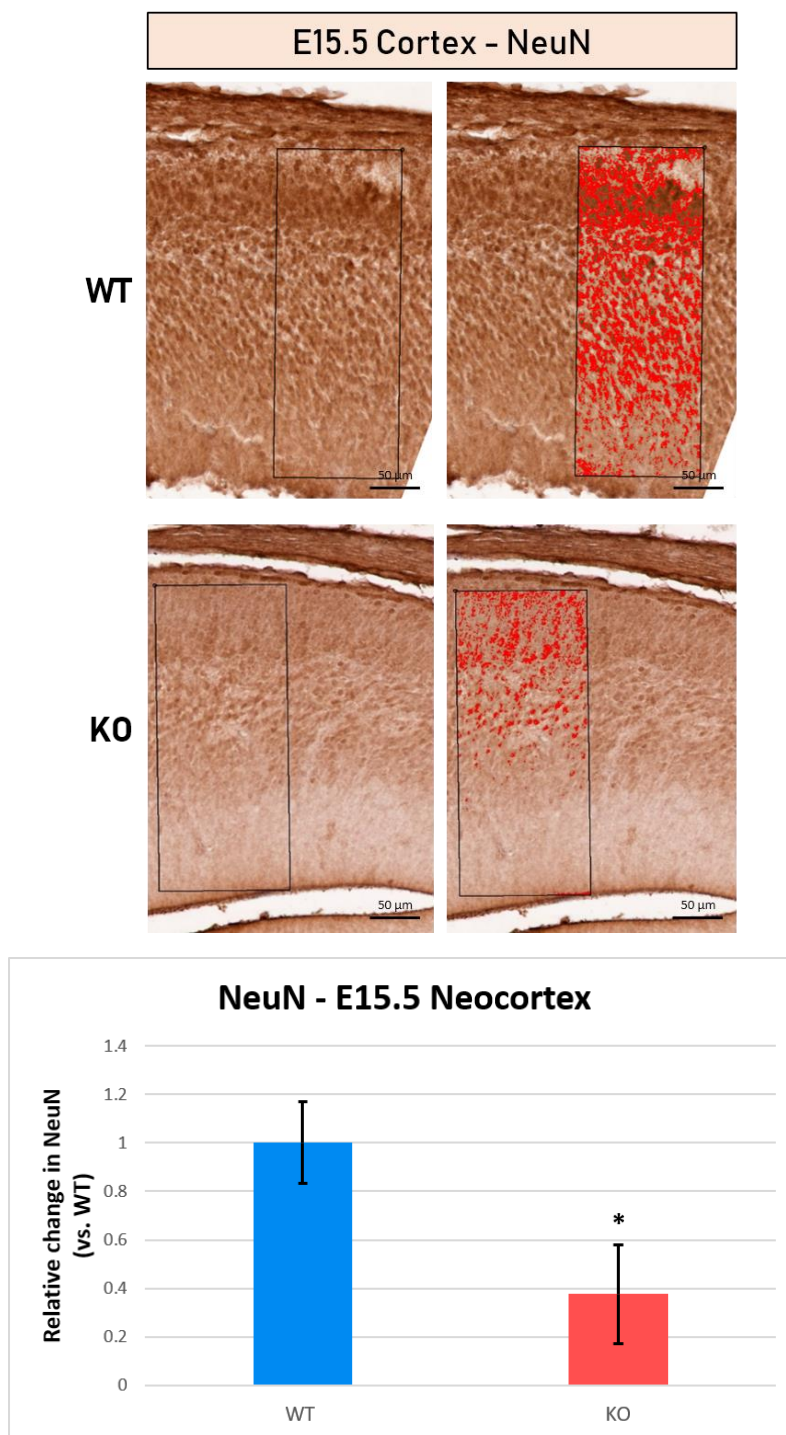
**Figure 16. E15.5 Cortex stained with NeuN.** Representative sections of E15.5 Cortex from WT (Top) and KO (Bottom) immunostained with mature neuron marker NeuN. The region of interest (ROI) and the specific antigen staining within the area has been highlighted and overlayed with red using cellSens software. With WT as 1, KO had about 0.4 of positive signal within same area of interest. Each data point was compared using unpaired t-test. Data are means +/- SEM of experiments performed in triplicate. *P<0.05. n=3

Chapter 4: Discussion

Previous findings from our lab illustrated involvement of *Spag17* in motile cilia and its central pair microtubule (38, 49). However, unexpected expression in the tissues without motile cilia like bone, and disrupted development in the absence of *Spag17* suggested that it might have broader influence (35). With the use of β-Gal assay and IHC, we were able to observe *Spag17* is also expressed throughout the development of the brain from embryonic day 11 and up to birth. This is consistent with anomalous brain phenotypes like hydrocephaly, corpus callosum and cerebellum underdevelopment presented on both on murine model and a patient with homozygous *Spag17* mutation (38, 48).

1) *Spag17* in cellular differentiation and maturation

Based on previously published data on *Spag17/CMV-Cre* KO showing changes in differentiation rate of chondrocytes and osteoblasts, we hypothesized that neural stem cells and neurons in the brain of *Spag17* KO will also have alternated differentiation rate. Consistent with our proposal, there was significant difference between WT and KO in relative area of positive signals for both NSC and mature neurons, signifying changes in differentiation. Via IHC on E15.5 and P0 WT and *Spag17* KO brain, we observed 1.5 to 2.5-fold increase in NSC and RGC positive signal in KO brain than WT, and mature neuron signal in KO brain being 60% less than WT. Similar trend was noted on the Glycogen Synthase Kinase 3 or GSK-3, a serine-threonine kinase that is heavily involved in regulating the transcription factor level in multiple signaling pathways (54). In their research, IHC on Gsk3-KO mice brain showed expansion of neural progenitor throughout rostro-caudal level, upregulated by 100-200% while number of mature neurons were decreased by 70% (54). Despite the increase in overall number of NSC and

progenitors like RGCs, number of mature cells being much less than the WT brains imply impeded neurogenesis process.

Right after exiting the mitotic cell cycle, immature neurons generated from NSC and RGCs need to go through subsequent maturation process before they start expressing mature neuronal cell markers (55). This newly formed neurons can be marked with antibodies against Tuj1, while more mature neurons can be highlighted with antibodies against MAP2 or NeuN. In the IHC performed on E15.5 WT and *Spag17/CMV-Cre* KO brain using Tuj1, we were able to observe a trend of more positive signal of immature neurons in KO than WT by 1.3 times. This phenomenon was also detected in the study done on *Arx*, a transcription factor that have been associated with neurodevelopmental disease including West Syndrome and lissencephaly both exhibiting mental retardation and spasmic episodes (55). In basal ganglia of mouse brain, they observed normal early differentiation from stem cell to immature neuron, but failure to mature or subsequent differentiation. Moreover, tangential migration and radial migration of those neurons were markedly reduced, leading to overall accumulation of immature neuron and decreased mature neuron in periventricular area (55). Even though our data did not have statistical significance, we prospect increasing sample numbers in future will show consistent trend with significance. Overall, combination of decreased mature neurons and buildup of immature neurons in *Spag17* KO uphold our initial hypothesis that *Spag17* plays critical role in neural cell differentiation and maturation, possibly hindering proper neurogenesis.

Interestingly, there have been comparable studies on changed rate of neurogenesis from overexpression or silencing of cytoskeletal gene similar to *Spag17*. In the study done on Tctex-1, a subunit of cytoplasmic dynein interacting with microtubule, silencing of the gene showed decrease in neural progenitor cells and increase in premature neuronal differentiation marked by

Tuj1 (56). Opposing the Tctex-1, overexpression of SPAG6, another protein associated with C1 microtubule of CPC, and known close and collaborator of SPAG17 led to inhibition of NSC proliferation and induced differentiation into neurons marked by Brn2 (57).

2) Conclusion and Future Directions

Our current findings support the premise that *Spag17* is important for cell differentiation and maturation. However, it is not yet known what is the mechanism of how this protein may play this role. Our lab has been studying this protein for several years and discovered that the protein may also be involved in primary cilia development. Primary cilia are an antenna like organelle that coordinates multiple morphogen signaling pathways and it is essential for developmental processes, in particular cell differentiation and maturation (4, 15, 58). In this context, future studies will investigate whether the role of *Spag17* in the development of the brain is associated with cell differentiation via a mechanism involving primary cilia. Future molecular studies will involve IHC on oligodendrocyte progenitor and astrocyte markers to see if non-neuronal cells differentiation rate is affected, western blot to confirm IHC and quantification data, and evaluation of primary cilia signaling pathways, including Wnt and HH signaling and the interaction with *Spag17*. Moreover, RNAseq studies in cells isolated from both WT and *Spag17* KO embryos at different stages will inform the transcriptional profile of these cells and how Wnt and HH signaling are regulated in the presence and absence of *Spag17*. Additional studies will evaluate the possible role of *Spag17* in the migration of cells during neuronal cell maturation and development.

References

1. Stiles, J., & Jernigan, T. L. (2010). The basics of brain development. *Neuropsychology review*, *20*(4), 327–348. doi:10.1007/s11065-010-9148-4

2. Gotz, M. & Huttner, W.B. (2005). The cell biology of neurogenesis. *Nature Review Molecular Cell Biology, 6*(10), 777-88. doi:10.1038/nrm1739

3. Dehay, C. & Kennedy, H. (2007). Cell-Cycle control and cortical development. *Nature Reviews Neuroscience, 8*(6), 438-50. doi:10.1038/nrn2097

4. Wilson, S. L., Wilson, J. P., Wang, C., Wang, B., & McConnell, S. K. (2012). Primary cilia and Gli3 activity regulate cerebral cortical size. *Developmental neurobiology*, *72*(9), 1196–1212. doi:10.1002/dneu.20985

5. Lim, S., & Kaldis, P. (2012). Loss of Cdk2 and Cdk4 induces a switch from proliferation to differentiation in neural stem cells. *Stem Cells, 30*(7), 1509-20. doi: 10.1002/stem.1114

6. Lehtinen, M. K., & Walsh, C. A. (2011). Neurogenesis at the brain-cerebrospinal fluid interface. *Annual Review of Cell and Developmental Biology, 27,* 653-79.

7. Chenn, A. & Walsh, C. (2002). Regulation of Cerebral Cortical Size by Control of Cell Cycle Exit in Neural Precursors. *Science, 297*, 365-369.

8. Homem, C. C., Repic, M., & Knoblich, J. A. (2015). Proliferation control in neural stem and progenitor cells. *Nature reviews. Neuroscience*, *16*(11), 647–659. doi:10.1038/nrn4021

9. Courchesne E., Mouton P. R., Calhoun M. E., Semendeferi K., Ahrens-Barbeau C., Hallet M. J., et al.. (2011). Neuron number and size in prefrontal cortex of children with autism. *JAMA 306*, 2001–2010. 10.1001/jama.2011.1638

10. Wegiel, J., Kuchna, I., Nowicki, K., Imaki, H., Wegiel, J., Marchi, E., … Wisniewski, T. (2010). The neuropathology of autism: defects of neurogenesis and neuronal migration, and

dysplastic changes. *Acta neuropathologica*, *119*(6), 755–770. doi:10.1007/s00401-010-0655-4

11. Geschwind, D. & Levitt, P. (2007). Autism spectrum disorders: developmental disconnection syndromes. *Current Opinion in Neurobiology, 17*(1), 103-111.

12. Tam, P., & Behringer, R. (1997). Mouse gastrulation: the formation of a mammalian body plan. *Mechanisms of Development, 68*(1-2), 3-25.

13. Purves D, Augustine GJ, Fitzpatrick D, et al., editors. (2001). *Neuroscience*. Sunderland, MA. Sinauer Associates. Available from: https://www.ncbi.nlm.nih.gov/books/NBK10993/

14. Gilthorpe, J. Papantoniou, E., …Wingate, R. (2002). The migration of cerebellar rhombic lip derivatives. *Development,129,* 4719-4728.

15. Spassky, N., Han, Y. G., Aguilar, A., Strehl, L., Besse, L., Laclef, C., … Alvarez-Buylla, A. (2008). Primary cilia are required for cerebellar development and Shh-dependent expansion of progenitor pool. *Developmental biology*, *317*(1), 246–259. doi:10.1016/j.ydbio.2008.02.026

16. Blom, H. J., Shaw, G. M., den Heijer, M., & Finnell, R. H. (2006). Neural tube defects and folate: case far from closed. *Nature reviews. Neuroscience*, *7*(9), 724–731. doi:10.1038/nrn1986

17. Taverna, E., Götz, M., & Huttner, W. (2014). The Cell Biology of Neurogenesis: Toward an Understanding of the Development and Evolution of the Neocortex. *Annual Reviews*, 30, 465-502.

18. Kriegstein, A., & Alvarez-Buylla, A. (2009). The glial nature of embryonic and adult neural stem cells. *Annual review of neuroscience*, *32*, 149-84.

19. Barry, D., Pakan, J., & McDermott, K. (2013). Radial Glial cells: Key organisers in CNS development. *The International Journal of Biochemistry & Cell Biology*, 46, 76-79.

20. Koblich, J. (2008). Mechanisms of Asymmetric Stem Cell Division. *Cell, 132*(4), 583-597.

21. Kessaris, N., Fogarty, M., Iannarelli, P., Grist, M., Wegner, M., & Richardson, W. D. (2005). Competing waves of oligodendrocytes in the forebrain and postnatal elimination of an embryonic lineage. *Nature neuroscience*, *9*(2), 173–179. doi:10.1038/nn1620

22. Rakic, P. (1972). Mode of Cell migration to the superficial layers of fetal monkey neocortex. *Journal of Comparative Neurology, 145*(1), 61-83.

23. Menezes, J. & Luskin, M. (1994). Expression of Neuron-Specific Tubulin Defines a Novel Population in the Proliferative Layers of the Developing Telencephalon. *The Journal of Neuroscience*, 14(9), 5399-5416.

24. Yao, B., & Jin, P. (2014). Unlocking epigenetic codes in neurogenesis. *Genes & Development, 28*(12), 1253–1271. doi:10.1101/gad.241547.114

25. Bystron, I., Blakemore, C., & Rakic, P. (2008). Development of the human cerebral cortex: Boulder Committee revisited. *Nature Reviews Neuroscience, 9*(2), 110-22

26. Higginbotham, H., Guo, J., Yokota, Y., Umberger, N. L., Su, C. Y., Li, J., … Anton, E. S. (2013). Arl13b-regulated cilia activities are essential for polarized radial glial scaffold formation. *Nature neuroscience*, *16*(8), 1000–1007. doi:10.1038/nn.3451

27. Guo, J., Higginbotham, H., Li, J., Nichols, J., Hirt, J., Ghukasyan, V., & Anton, E. S. (2015). Developmental disruptions underlying brain abnormalities in ciliopathies. *Nature communications, 6,* 7857. doi:10.1038/ncomms8857

28. Reemst, K., Noctor, S. C., Lucassen, P. J., & Hol, E. M. (2016). The Indispensable Roles of Microglia and Astrocytes during Brain Development. *Frontiers in human neuroscience*, *10*, 566. doi:10.3389/fnhum.2016.00566

29. Ge, W. P., Miyawaki, A., Gage, F. H., Jan, Y. N., & Jan, L. Y. (2012). Local generation of glia is a major astrocyte source in postnatal cortex. *Nature, 484*(7394), 376–380. doi:10.1038/nature10959

30. Goldman, S. A., & Kuypers, N. J. (2015). How to make an oligodendrocyte. Development (Cambridge, England), 142(23), 3983–3995. doi:10.1242/dev.126409 Eriksson, P.S., Perfillieva, E., …Gage, F.H. (1998). Neurogenesis in the adult human hippocampus. *Nature Medicine, 4*(11), 1313-7.

31. Merkle, F. T., Tramontin, A. D., García-Verdugo, J. M., & Alvarez-Buylla, A. (2004). Radial glia give rise to adult neural stem cells in the subventricular zone. *Proceedings of the National Academy of Sciences of the United States of America*, *101*(50), 17528–17532. doi:10.1073/pnas.0407893101

32. Miron V., Kuhlmann, T., & Antel J. (2011). Cells of the oligodendroglial lineage, myelination, and remyelination. *Biochimica et Biophysica Acta*, 1812 (2), 184-93. doi: 10.1016/j.bbadis.2010.09.010

33. Barazzuol, L., Rickett, N., Ju, L., & Jeggo, P. A. (2015). Low levels of endogenous or X-ray-induced DNA double-strand breaks activate apoptosis in adult neural stem cells. *Journal of cell science*, *128*(19), 3597–3606. doi:10.1242/jcs.171223

34. Zhang Z., Jones B.H., Tang W., Moss S.B., Wei Z., Ho C., Pollack M., Horowitz E., Bennett J., Baker M.E., et al. (2005). Dissecting the Axoneme Interactome: The Mammalian Orthologue of Chlamydomonas PF6 Interacts with Sperm-Associated Antigen 6, The

Mammalian Orthologue of Chlamydomonas PF6. *Mol. Cell. Proteom.4,* 914–923. doi: 10.1074/mcp.M400177-MCP200.

35. Teves, M. E., Sundaresan, G., Cohen, D. J., Hyzy, S. L., Kajan, I., Maczis, M., … Strauss, J. F. (2015). *Spag17* deficiency results in skeletal malformations and bone abnormalities. *PloS one*, *10*(5), e0125936. doi:10.1371/journal.pone.0125936

36. Teves, M. E., Nagarkatti-Gude, D. R., Zhang, Z., & Strauss, J. F. (2016). Mammalian axoneme central pair complex proteins: Broader roles revealed by gene knockout phenotypes. *Cytoskeleton (Hoboken, N.J.)*, *73*(1), 3–22. doi:10.1002/cm.21271

37. Goduti, D. J., & Smith, E. F. (2012). Analyses of functional domains within the PF6 protein of the central apparatus reveal a role for PF6 sub-complex members in regulating flagellar beat frequency. *Cytoskeleton (Hoboken, N.J.), 69*(3), 179–194. doi:10.1002/cm.21010

38. Teves, M. E., Zhang, Z., Costanzo, R. M., Henderson, S. C., Corwin, F. D., Zweit, J., … Strauss, J. F. (2013). Sperm-associated antigen-17 gene is essential for motile cilia function and neonatal survival. *American Journal of Respiratory Cell and Molecular Biology, 48*(6), 765–772. doi:10.1165/rcmb.2012-0362OC

39. Lee, L. (2011). Mechanisms of mammalian ciliary motility: Insights from primary ciliary dyskinesia genetics. *Gene, 473*(2), 57-66.

40. Weedon MN, Frayling TM (2008) Reaching new heights: insights into the genetics of human stature. *Trends Genet 24*: 595–603.

41. Weedon, M. N., Lango, H., Lindgren, C. M., Wallace, C., Evans, D. M., Mangino, M., … Frayling, T. M. (2008). Genome-wide association analysis identifies 20 loci that influence adult height. *Nature genetics*, *40*(5), 575–583. doi:10.1038/ng.121

42. Takeuchi F, Nabika T, Isono M, Katsuya T, Sugiyama T, Yamaguchi S, Kobayashi S, et al. (2009). Evaluation of genetic loci influencing adult height in the Japanese population. *Journal of Human Genetics, 54*. 749–752

43. Zhao, J., Li, M., Bradfield, J. P., Zhang, H., Mentch, F. D., Wang, K., … Grant, S. F. (2010). The role of height-associated loci identified in genome wide association studies in the determination of pediatric stature. *BMC medical genetics*, *11*, 96. doi:10.1186/1471-2350-11-96

44. N'Diaye, A., Chen, G. K., Palmer, C. D., Ge, B., Tayo, B., Mathias, R. A., … Haiman, C. A. (2011). Identification, replication, and fine-mapping of Loci associated with adult height in individuals of african ancestry. *PLoS genetics*, *7*(10), e1002298. doi:10.1371/journal.pgen.1002298

45. van der Valk, R. J., Kreiner-Møller, E., Kooijman, M. N., Guxens, M., Stergiakouli, E., Sääf, A., … Early Growth Genetics (EGG) Consortium (2014). A novel common variant in DCST2 is associated with length in early life and height in adulthood. *Human molecular genetics*, *24*(4), 1155–1168. doi:10.1093/hmg/ddu510

46. Wood, A. R., Esko, T., Yang, J., Vedantam, S., Pers, T. H., Gustafsson, S., … Frayling, T. M. (2014). Defining the role of common variation in the genomic and biological architecture of adult human height. *Nature genetics*, *46*(11), 1173–1186. doi:10.1038/ng.3097

47. Kim J. J., Lee H. I., Park T., Kim K., Lee J. E., Cho N. H., et al. (2010). Identification of 15 loci influencing height in a Korean population. J. Hum. Genet. 55 27–31. 10.1038/jhg.2009.116

48. Córdova-Fletes C., Becerra-Solano L.E., Rangel-Sosa M.M., Rivas-Estilla A.M., Alberto Galán-Huerta K., Ortiz-López R., Rojas-Martínez A., Juárez-Vázquez C.I., García-Ortiz J.E.

(2017). Uncommon runs of homozygosity disclose homozygous missense mutations in two ciliopathy-related genes (SPAG17 and WDR35) in a patient with multiple brain and skeletal anomalies. *European Journal of Medical Genetics, 61*(3), 161–167.

49. Kazarian, E., Son, H., Sapao, P., Li, W., Zhang, Z., Strauss, J. F., & Teves, M. E. (2018). SPAG17 Is Required for Male Germ Cell Differentiation and Fertility. *International journal of molecular sciences*, *19*(4), 1252. doi:10.3390/ijms19041252 ?

50. Michalcczyk, K. & Ziman, M. (2005). Nestin structure and predicted function in cellular cytoskeletal organization. *Histology and Histopathology*, *20*, 665-671.

51. Gomez-Climent, M., Guirado, R., Varea, E., & Nacher, J. (2010). "Arrested development". Immature, but not recently generated, neurons in the adult brain. *Archives Italiennes de Biologie, 148*, 159-172.

52. Mullen, R.J., Buck, C.R., & Smith, A.M. (1992). NeuN, a neuronal specific nuclear protein in vertebrates. *Development*, 116(1). 201-11.

53. Gusel'nikova, V. V., & Korzhevskiy, D. E. (2015). NeuN As a Neuronal Nuclear Antigen and Neuron Differentiation Marker. *Acta naturae*, *7*(2), 42–47.

54. Kim, W. Y., Wang, X., Wu, Y., Doble, B. W., Patel, S., Woodgett, J. R., & Snider, W. D. (2009). GSK-3 is a master regulator of neural progenitor homeostasis. Nature neuroscience, 12(11), 1390–1397. doi:10.1038/nn.2408

55. Colombo, E., Collombat, P., Colasante, G., Bianchi, M., Long, J., Mansouri, A., … Broccoli, V. (2007). Inactivation of Arx, the murine ortholog of the X-linked lissencephaly with ambiguous genitalia gene, leads to severe disorganization of the ventral telencephalon with impaired neuronal migration and differentiation. *The Journal of Neuroscience, 27*(17), 4786–4798. doi:10.1523/JNEUROSCI.0417-07.2007

56. Li, A., Saito, M., Chuang, J. Z., Tseng, Y. Y., Dedesma, C., Tomizawa, K., … Sung, C. H. (2011). Ciliary transition zone activation of phosphorylated Tctex-1 controls ciliary resorption, S-phase entry and fate of neural progenitors. *Nature cell biology, 13*(4), 402–411. doi:10.1038/ncb2218

57. Hu X, Yan R, Cheng X, Song L, Zhang W, Li K, & Zhao, S. (2016). The function of sperm-associated antigen 6 in neuronal proliferation and differentiation. *J. Mol. Histol. 47*(6). 531–540. doi: 10.1007/s10735-016-9694-z.

58. Singla, V. & Reiter, J. (2006). The Primary Cilium as the Cell's Antenna: Signaling at a Sensory Organelle. *Science, 313*. 629-633.

Vita

Olivia Jeong Min Choi was born on June 29, 1993 in Daegu, Republic of Korea. She moved to United States in 2005 and received her Bachelor of Science in Forensic Science and minor in Biology at George Mason University in Fairfax, Virginia on Dec 2016. Olivia then moved to Richmond, VA to attend VCU for Premedical Graduated Health Sciences Certificate Program and continued on earning M.S in Physiology and Biophysics at VCU under Dr. Maria Teves.